Size manipulation of metal particles with laser light

M. Vollmer, R. Weidenauer, W. Hoheisel, U. Schulte, and F. Träger
Physikalisches Institut der Universität Heidelberg, Philosophenweg 12, D-6900 Heidelberg 1, Federal Republic of Germany
(Received 23 August 1989)

It is demonstrated that the size of small metal particles can be manipulated with laser light. Even a considerable narrowing of a given size distribution on a surface can be achieved. This becomes possible by a size-selective laser-ablation process. Besides measurements of the ablation rate as a function of illumination time, laser wavelength, laser intensity, and particle size, a model is presented for the variation of the size distribution. Good agreement with experiment is found.

The physics and chemistry of clusters and especially the study of metal clusters supported on surfaces has found increasing interest in recent years.[1] Many experiments are motivated by the prospect of possible applications and a better understanding of technological processes already involving clusters. Examples are heterogeneous catalysis, photography, or the generation of thin films, just to name a few. On the other hand, research in this field addresses the change of fundamental physical and chemical properties as a function of particle size. One of the key issues for such measurements as well as for technological applications is the generation of particles with well-defined size and narrow size distributions. The present paper demonstrates that the size of small metal particles can be manipulated in a well-defined way with laser light. Even a considerable narrowing of a given distribution on a surface can be achieved. This becomes possible by a laser "photon sputtering" or ablation process which can be controlled such that particles in a certain size range shrink selectively as a result of an ongoing removal of atoms from their surfaces. In addition to measurements of the ablation rate as a function of illumination time, laser wavelength, laser intensity, and particle size, a model is presented for the variation of the size distribution.

In our experiments metal particles are generated on a LiF(100) single-crystal surface in ultrahigh vacuum by deposition of sodium atoms and subsequent surface diffusion.[2] This gives a size distribution with a width of typically one-third to one-half of the average particle size.[3] The mean particle size is determined by measuring the decreasing rate of inelastically scattered atoms during the deposition.[2] The particles are illuminated with light of an argon or krypton ion laser. As a result, individual atoms are ejected from the surface of the particles. They are detected with a quadrupole mass spectrometer. The underlying *nonthermal* desorption process has been described recently and is based on surface plasmon excitation.[4] It has two important features that make a specific variation of the particle size possible. First, the surface plasmon excitation exhibits a resonance as a function of laser frequency. Second, the transition frequency of this resonance depends on the particle size. As a consequence, a resonant dependence of the ablation rate on the cluster radius occurs which is different for different laser wavelengths. The result of such a measurement is shown in Fig. 1. If green laser light with $\lambda=514$ nm is chosen, for example, particles with mean radii of $R_0=45$ nm interact preferably, eject atoms, and shrink under continuous illumination. As a result, the size distribution changes. The ablation naturally comes to an end if the size of the particles has decreased so much that they are shifted out of resonance. In general, a given distribution on a surface can be manipulated in different ways depending on the chosen laser frequency and on the average particle size. This will be illustrated in detail below.

A model has been developed to describe this size manipulation quantitatively. For a fixed laser wavelength λ the absorption resonance curve as a function of radius is approximated by a Gaussian centered at R_λ. The assumption of a symmetrical absorption profile is supported by experimental and theoretical work on plasma resonances of particles in matrices.[5] The cluster size distribution $f(R)$ is asymmetrical[3] and is approximated by a superposition of two half Gaussians of different widths, which are centered at R_0. The number of desorption sites on a cluster of radius R is written as aR where a is a

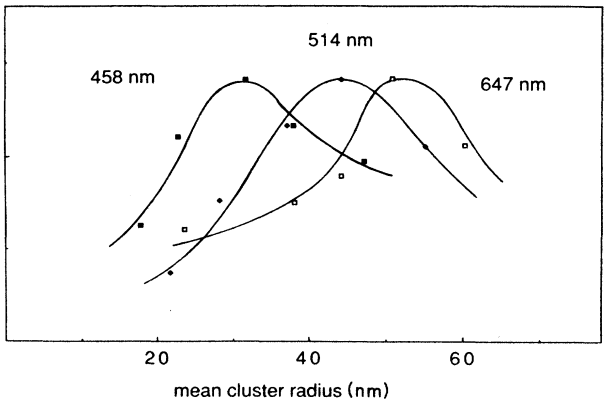

FIG. 1. Dependence of the normalized laser-induced ablation signal on the mean particle radius for fixed laser wavelengths of $\lambda=458$, 514, and 647 nm.

constant that depends on the shape of the cluster.[6] With these parameters the ablation rate dN/dt originating from particles in the size interval $[R, R+\Delta R]$ at time t can be expressed as

$$\frac{dN}{dt} = \sigma_0 I a N_c Q f(R) R \exp\left[-\frac{(R-R_\lambda)^2}{2\beta^2}\right]\Delta R \ . \quad (1)$$

σ_0 is the cross section for absorption of light at $R=R_\lambda$, I is the number of incident photons per cm^2 s, N_c the number of illuminated clusters, Q the quantum efficiency, and β the width of the absorption profile. As a first step the desorption rate was calculated for each size interval ΔR. From this the resulting changes of the particle radii were computed. The time dependence of the distribution $f(R)$ during continuous laser irradiation was obtained by integration over the actual size distribution and iterative application of the procedure outlined above. The numerical computation has been carried out for different particle sizes, excitation frequencies, and laser intensities. Two examples will be described here. In the first one the wavelength of the incident laser light was $\lambda=514$ nm. An absorption resonance curve which peaks at 45 nm (see Fig. 1) and has a full width at half maximum (FWHM) of 21 nm (Ref. 5) was used. The mean cluster radius of the initial distribution was $R_0=42$ nm with a FWHM of 22 nm. Figure 2 displays the calculated ablation rates for two laser intensities of $I=100$ and 15 W/cm^2 and the corresponding change of the size distribution as a function of irradiation time. The different traces (dashed lines) refer to the distribution assumed initially on the surface (0) and obtained 30 s (1), 60 s (2), 90 s (3), and 120 s (4) after starting the illumination with laser light, respectively ($I=100$ W/cm^2). After 120 s, 72% of the total coverage has desorbed. Included is also the assumed absorption profile (solid line) for light of $\lambda=514$ nm. Figure 3 depicts the results for the second example in which different values for both the laser wavelength ($\lambda=488$ nm) and the mean particle size ($R_0=62$ nm) were chosen.

As can be seen from Figs. 2(a) and 3(a), the ablation rate exhibits very different dependencies as a function of illumination time. A monotonous decrease [see Fig. 2(a)], but also an initial rise followed by a maximum and a decrease [see Fig. 3(a)] may take place. Also, the change of the distribution can be very different. For $R_0=42$ nm and $\lambda=514$ nm, it is shifted to smaller particle radii and becomes narrower. Conversely, a depletion in one of the wings takes place for an initial mean size of $R_0=62$ nm and $\lambda=488$ nm [Fig. 3(b)]. Simultaneously, a second narrow peak at smaller particle radii grows.

In general, the dependence of the ablation rate as a function of irradiation time and the resulting variation of the size distribution is the interplay of two effects. First, the number of atoms which can desorb decreases as a function of time due to the overall decrease of the surface coverage. Second, the ablation results in a shift of the particle size in or out of resonance depending on the relative position of the distribution and the absorption profile. The above examples can therefore be interpreted as follows. For $R_0=42$ nm and $\lambda=514$ nm, the absorption profile [solid line in Fig. 2(b)] of the plasma resonance overlaps almost completely with the size distribution so that most of the clusters interact with the laser light. They eject atoms, shrink, and are shifted out of resonance. Consequently, the ablation rate decreases as a function of time [see Fig. 2(a)]. Since there is a gradient of the absorption cross section over the width of the particle distribution, a considerable narrowing of the size distribution takes place. Figure 2(b) shows that this narrowing is as large as a factor of 6 after 120 s. It proceeds further if the illumination is continued and can easily amount to a factor of 10. For $R_0=62$ nm and $\lambda=488$ nm, on the other hand, the initial size distribution is shifted with respect to the absorption profile [see Fig. 3(b)] and only a small fraction of the particles can undergo ablation. Those clusters that interact with the light become smaller and are shifted *across* the absorption profile. They first interact more and more efficiently with

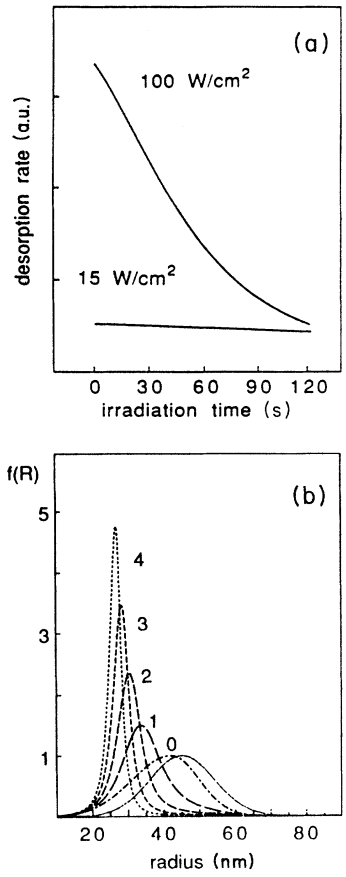

FIG. 2. Calculated change of the ablation rate (a) and the corresponding change of the particle size distribution (b) during laser illumination with $\lambda=514$ nm. The initial average cluster size was $R_0=42$ nm with a FWHM of 22 nm. The rate was calculated for two different laser intensities of $I=100$ W/cm^2 and $I=15$ W/cm^2. The different traces in (b) (dashed lines) refer to the distribution assumed initially on the surface (0) and obtained 30 s (1), 60 s (2), 90 s (3), and 120 s (4) after starting the illumination ($I=100$ W/cm^2), respectively. Included is also the absorption profile (solid line, lower panel) for light of $\lambda=514$ nm.

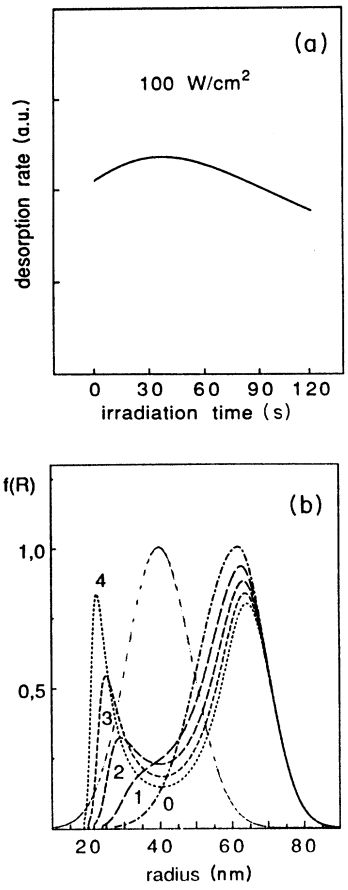

FIG. 3. Calculated change of the ablation rate (a) and the corresponding change of the particle size distribution (b) during laser illumination with $\lambda=488$ nm and $I=100$ W/cm^2. The initial average cluster size was $R_0=62$ nm with a FWHM of 22 nm. The different traces in (b) (dashed lines) refer to the distribution assumed initially on the surface (0) and obtained 30 s (1), 60 s (2), 90 s (3), and 120 s (4) after starting the illumination, respectively. Included is also the absorption profile (solid line, lower panel) for light of $\lambda=488$ nm.

the light and the ablation rate increases until they have reached the maximum of the resonance [see Fig. 3(a)]. Similar to the first example discussed above, the particles are subsequently shifted out of resonance and the rate decreases. As a consequence, a second maximum in the distribution develops.

As can be seen from Eq. (1), the change of the size distribution is intimately correlated to the variation of the ablation rate as a function of illumination time. Indeed, the time dependence of the rate directly reflects the variation of the size distribution. Therefore the model can be tested and the change of the distribution verified experimentally by measuring the desorption rate and its change for different experimental conditions. Such a test is particularly meaningful since the time dependence of the ablation rate exhibits pronounced differences characteristic of the chosen conditions [see Figs. 2(a) and 3(a)]. To test the model we have therefore recorded the ablation rates

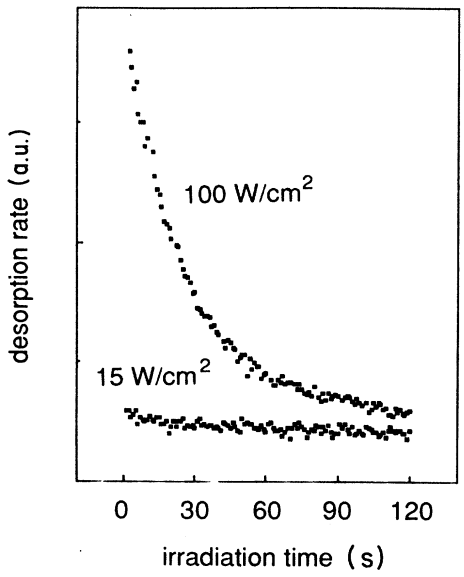

FIG. 4. Experimental ablation rates as a function of irradiation time with laser light. The experimental conditions were identical to those of Fig. 2 with $\lambda=514$ nm, an initial average particle size of $R_0=42$ nm, and laser intensities of $I=100$ W/cm^2 and $I=15$ W/cm^2.

for a variety of laser-frequency–cluster-radius combinations, particularly for the particle sizes and absorption profiles used in the above examples. The results are shown in Figs. 4 and 5. In Fig. 4 the average initial cluster size was $R_0=42$ nm and the clusters were illuminated by laser light of $\lambda=514$ nm with an intensity of $I=100$

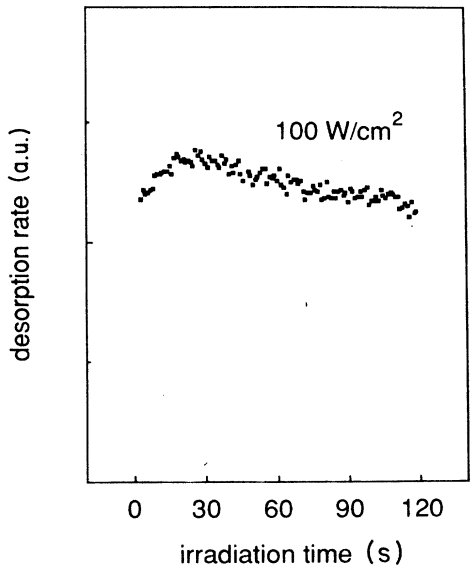

FIG. 5. Experimental ablation rate as a function of irradiation time with laser light. The experimental conditions were identical to those of Fig. 3 with $\lambda=488$ nm, an initial average particle size of $R_0=62$ nm, and a laser intensity of $I=100$ W/cm^2.

W/cm^2. In agreement with the theoretical prediction, a decrease of the rate is observed starting at the very beginning of the illumination. The slope of the decrease depends upon the light intensity since the ablation proceeds slower for low ($I=15$ W/cm^2) as compared to high ($I=100$ W/cm^2) intensities (see Fig. 4). Again, this is in good agreement with the model calculation. Figure 5 shows the results of a measurement in which the absorption profile and the size distribution are shifted with respect to each other. The laser wavelength was $\lambda=488$ nm and the average initial cluster size was $R_0=62$ nm. The rate now exhibits an increase followed by a maximum and a decrease. This is also reproduced by the theoretical result (see Fig. 3). The position of the maximum sensitively depends upon the light intensity. For small intensities the signals increase slowly and have the maximum at very large irradiation times. For high intensities, on the other hand, the rate changes are very pronounced and the maximum is reached in a short period of time. An additional argument in favor of the size manipulation is based on a comparison of the experimental and theoretical desorption yield. Again, we find that the experimental value is reproduced by the theoretical model.

The excellent agreement of the theoretical predictions with experiment for many different sets of parameters provides convincing evidence for the validity of the presented model and for the manipulation of the cluster size distribution under illumination with laser light. In general, the described size manipulation should be possible for all metal particles where the binding energy of a surface atom is smaller than the absorbed photon energy. Future experiments include the possibility to manipulate the size distribution by subsequent irradiation with different laser wavelengths to tailor clusters with very special distributions. Furthermore, applications of such particles for purposes like catalysis offer interesting perspectives. At present, experiments on silver particles including *in situ* electron microscopy are under preparation in our laboratory.

[1]*Metal Clusters,* edited by F. Träger and G. zu Putlitz (Springer, Heidelberg, 1986); *Metal Clusters,* edited by M. Moskovits (Wiley, New York, 1986); W. P. Halperin, Rev. Mod. Phys. **58**, 533 (1986); W. A. de Heer, W. D. Knight, M. Y. Chou, and M. L. Cohen, Solid State Phys. **40**, 93 (1987).

[2]M. Vollmer and F. Träger, Z. Phys. D **3**, 291 (1986).

[3]H. Poppa, J. Vac. Sci. Technol. **2**, 42 (1965); H. Schmeisser, Thin Solid Films **22**, 83 (1974).

[4]W. Hoheisel, K. Jungmann, M. Vollmer, R. Weidenauer, and F. Träger, Phys. Rev. Lett. **60**, 1649 (1988); W. Hoheisel, U. Schulte, M. Vollmer, R. Weidenauer, and F. Träger, Appl. Surf. Sci. **36**, 664 (1989).

[5]J. A. A. J. Perenboom. P. Wyder, and F. Meier, Phys. Rep. **78**, 171 (1981); U. Kreibig and L. Genzel, Surf. Sci. **156**, 678 (1985).

[6]M. Vollmer and F. Träger, Surf. Sci. **187**, 445 (1987).